Raster-Scanning Optoacoustic Mesoscopy for Gastrointestinal Imaging at High Resolution

Ferdinand Knieling,[1,2] Jean Gonzales Menezes,[2] Jing Claussen,[3] Mathias Schwarz,[3] Clemens Neufert,[2] Fabian B. Fahlbusch,[1] Timo Rath,[2,4] Oana-Maria Thoma,[2,5] Viktoria Kramer,[2] Bianca Menchicchi,[2] Christina Kersten,[2] Kristina Scheibe,[2] Sebastian Schürmann,[6] Birgitta Carlé,[6] Wolfgang Rascher,[1] Markus F. Neurath,[2,4] Vasilis Ntziachristos,[7,8] and Maximilian J. Waldner[2,5]

[1]Department of Pediatrics and Adolescent Medicine, [2]Department of Medicine 1, Friedrich-Alexander-Universität Erlangen-Nürnberg, [3]iThera Medical GmbH, München, [4]Ludwig Demling Center of Excellence, Friedrich-Alexander-Universität Erlangen-Nürnberg, [5]Erlangen Graduate School in Advanced Optical Technologies (SAOT), [6]Institute of Medical Biotechnology, Friedrich-Alexander-Universität Erlangen-Nürnberg, Nürnberg, [7]Institute for Biological and Medical Imaging, Helmholtz Zentrum München, [8]Chair for Biological Imaging, TranslaTUM, Technische Universität München, München, Germany

This article has an accompanying continuing medical education activity, also eligible for MOC credit, on page e15. Learning Objective: Upon completion of this CME exercise, successful learners will be able to evaluate the potential of raster-scanning optoacoustic mesoscopy for gastrointestinal imaging.

In vivo optical imaging modalities are mostly limited to cell cultures, superficial tissues, and intravital imaging since they lack either resolution or penetration depth.[1] In contrast, optoacoustic (OA) imaging—combining features of optical and ultrasound imaging—has been used to visualize hemoglobin in depths of approximately 3 cm in patients with Crohn's disease.[2,3] Realizing an even higher resolution, raster-scanning OA mesoscopy (RSOM) provides intrinsic optical tissue contrast down to 10-20 μm resolution at still high penetration depths of several millimeters.[4,5] In this article, with its accompanying videos, we demonstrate the capability of RSOM to perform high resolution in vivo gastrointestinal imaging and explore its potential clinical use.

Description of the Technology

The imaging technology is integrated into a OA small animal scanner that builds on a RSOM system (RSOM Explorer P50, iThera Medical GmbH, München, Germany; Figure 1*B*).[5,6] It uses a custom-made spherically focused LiNbO3 detector (center frequency, 50 MHz; bandwidth, 10-90 MHz; focal diameter, 3 mm; focal distance, 3 mm; f-number, 1). The recorded data are amplified by a low noise amplifier of 63-dB gain. The illumination is generated by a 532-nm diode pumped solid state laser (pulses, 1 ns; $\leq$1 mJ/pulse; repletion rate, 2 kHz). The laser light is delivered through a customized 2-arm fiber bundle (spot size, 3.5 $\times$ 5 mm). The scanning head is attached to 2 motorized stages, enabling raster scanning over a field of view of $\leq$15 $\times$ 15 mm (step size, 20 μm). The scan head is coupled to the sample surface by an interchangeable water-filled (2 mL) interface. The recorded data are reconstructed with a beam-forming algorithm, which models the sensitivity field of the focused detector.[6–8]

Video Description

The first video gives an overview of light- and soundwave-based imaging technologies that are used currently or in translation for high-resolution imaging. It explains how RSOM combines optical and ultrasound imaging to provide excellent specifications for preclinical and translational gastrointestinal imaging.

Then, the principle of OA imaging is explained. It is based on the illumination of tissue with pulsed laser light at 532 nm. The light gets absorbed by tissue chromophores, which undergo thermoelastic expansion followed by the generation of pressure waves that are detected. Taking a freshly excised liver as an example, we demonstrate the ability of RSOM to visualize the vasculature of organs (green, small vessels; red, big vessels) without any label (Figure 1*C–E*).

In the second video, we show label-free images of freshly excised murine colons bearing inflammation and tumors to visualize neovascularization in neoplastic tissues. The

Abbreviations used in this paper: **OA, optoacoustic; RSOM, raster-scanning optoacoustic mesoscopy.**

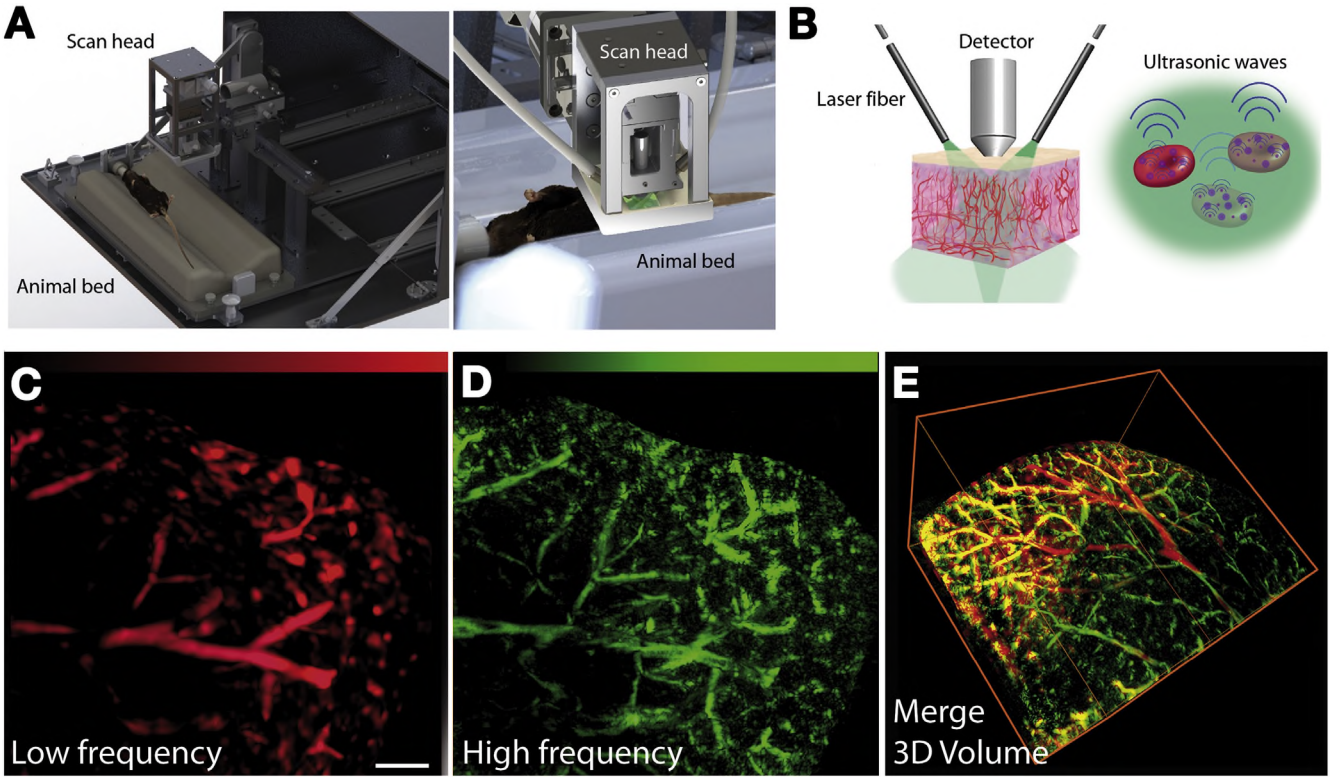

Figure 1. (*A*) Technical setup. (*B*) Imaging principle. (*C*) Low-frequency (10-30MHz) detection of freshly excised liver tissue. (*D*) High-frequency (30-90MHz) detection. (*E*) Three-dimensional volume overlay. Bars, 1 mm; XY-box, 8 mm.

capability of RSOM for noninvasive in vivo transabdominal imaging in mice is demonstrated. The increased vasculature of the colon wall during inflammation is compared to healthy specimen (Figure 2*A*–D). In an adoptive T-cell transfer colitis model, we provide the evidence that RSOM could noninvasively detect structures resembling injected labeled T cells infiltrating into the colon wall of mice with colitis.

Take Home Message

We demonstrate that RSOM allows noninvasive imaging at high resolution in vivo. In contrast with other optical imaging

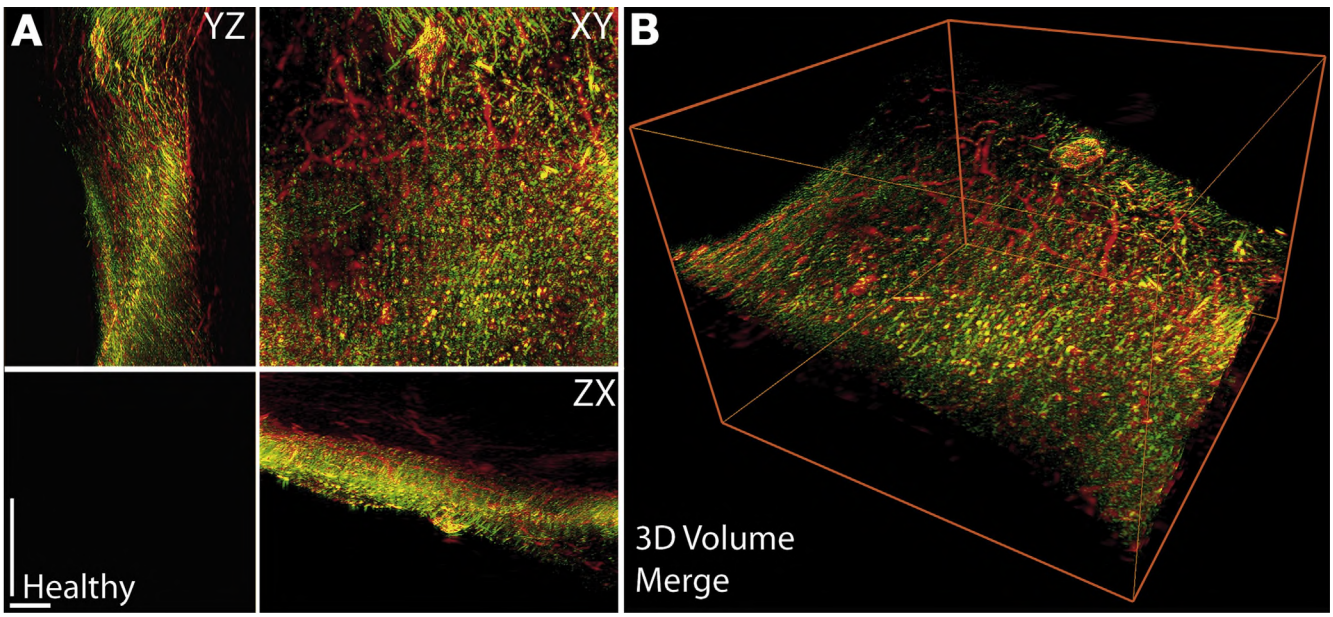

Figure 2. In vivo raster-scanning optoacoustic mesoscopy imaging from healthy and inflamed mice. The images are reconstructed from single image planes of the murine colon (maximum depth, 3 mm). Detected signals originate from hemoglobin (10-90 MHz). (*A*) In vivo imaging from healthy mice. Full projections (FP) YZ, XY, and XZ. (*B*) Three-dimensional volume. (*C*) In vivo imaging from colitis; FP YZ, XZ, and XZ. (*D*) Three-dimensional volume. Bars, 1 mm; XY-box, 8 mm.

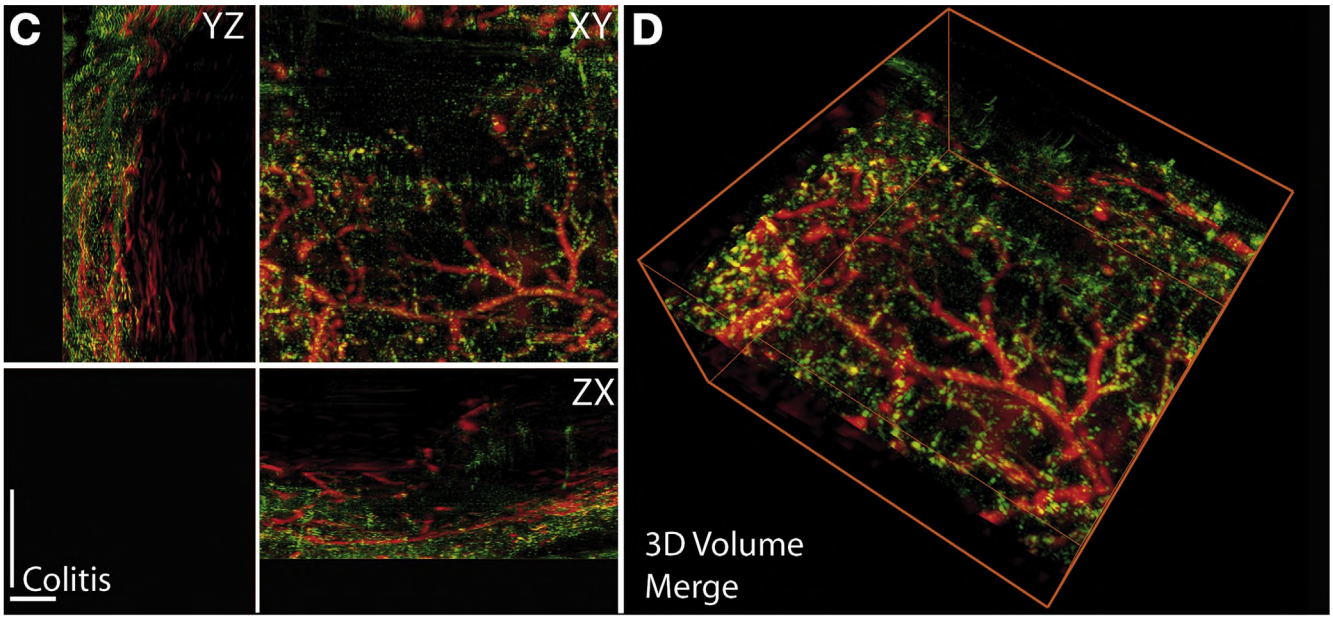

Figure 2. Continued

modalities, this technology is not generally restricted to the application of exogenous dyes. Because we used a single wavelength laser for illumination, the integration of multiple wavelengths could further enable the label-free determination of hemoglobin oxygenation, of further tissue molecules (eg, collagens), and a broader range of fluorescent dyes or proteins.

In the future, the integration in endoscopic devices might allow the label-free visualization of multiple, deeper layers of the intestinal wall at single cell resolution.

Supplementary Material

Note: To access the supplementary material accompanying this article, visit the online version of *Gastroenterology* at www.gastrojournal.org, and at https://doi.org/10.1053/j.gastro.2017.11.285.

References

1. Ntziachristos V. Going deeper than microscopy: the optical imaging frontier in biology. Nat Methods 2010; 7:603–614.
2. Knieling F, Neufert C, Hartmann A, et al. Multispectral optoacoustic tomography for assessment of Crohn's disease activity. N Engl J Med 2017;376:1292–1294.
3. Waldner MJ, Knieling F, Egger C, et al. Multispectral optoacoustic tomography in Crohn's disease: noninvasive imaging of disease activity. Gastroenterology 2016; 151:238–240.
4. Ntziachristos V, Razansky D. Molecular imaging by means of multispectral optoacoustic tomography (MSOT). Chem Rev 2010;110:2783–2794.
5. Omar M, Schwarz M, Soliman D, et al. Pushing the optical imaging limits of cancer with multi-frequency-band raster-scan optoacoustic mesoscopy (RSOM). Neoplasia 2015;17:208–214.
6. Omar M, Soliman D, Gateau J, et al. Ultrawideband reflection-mode optoacoustic mesoscopy. Opt Lett 2014;39:3911–3914.
7. Schwarz M, Soliman D, Omar M, et al. Optoacoustic dermoscopy of the human skin: tuning excitation energy for optimal detection bandwidth with fast and deep imaging in vivo. IEEE Trans Med Imaging 2017; 36:1287–1296.
8. Schwarz M, Buehler A, Ntziachristos V. Isotropic high resolution optoacoustic imaging with linear detector arrays in bi-directional scanning. J Biophotonics 2015; 8:60–70.

Reprint requests
Address requests for reprints to: Maximilian J. Waldner, MD, Department of Medicine 1, Friedrich-Alexander-Universität Erlangen-Nürnberg, Ulmenweg 18, 91054 Erlangen, Germany. e-mail: maximilian.waldner@uk-erlangen.de.

Acknowledgements
O.M.T. and M.J.W. gratefully acknowledges funding of the Erlangen Graduate School in Advanced Optical Technologies (SAOT) by the German Research Foundation (DFG) in the framework of the German excellence initiative, and funding by the German Research Foundation (DFG) within the Klinische Forschergruppe 257 (KFO 257) and Forschergruppe 2438 (FOR 2438). M.F.N. gratefully acknowledges funding by the Emerging Fields Initiative of the Friedrich-Alexander-Universität Erlangen-Nürnberg and by the German Research Foundation (DFG) within Collaborative Research Center 1181 "Checkpoints for resolution of inflammation." This project has received funding from the European Union's Horizon 2020 research and innovation program under grant agreement No 732720 (ESOTRAC). The authors thank Andrea Hartner for support during study execution.

Conflicts of interest
The authors disclose no conflicts.

J.C. and M.S. are employees of iThera Medical. All other authors disclose no conflicts of interest. Activities not related to the article: F.K. and M.J.W. received travel expenses for scientific meetings from iThera Medical GmbH, Germany. V.N. is a shareholder of iThera Medical. Other relationships: V.N. has US 20140198606 A1 / EP2754388A1, WO 2012103903 A1, WO 2011000389 A1, EP2148183, PCT/EP2008/006142, and US 61/066,187; PCT/EP2009/001137 patents issued and patent WO201109810 1A1, PCT/EP2010/006937 licensed by SurgOptics B.V.

Tissue Preparation

For fresh tissue, C57B6/J mice were humanely killed and organs were immediately transferred into phosphate buffered saline (PBS; Sigma-Aldrich Chemie GmbH, Munich, Germany). Raster-scanning optoacoustic mesoscopy (RSOM) imaging was performed without any further preparation and within <1 hour.

Isolation of Primary Cells

$CD4^+CD25^-$ T cells were isolated from murine splenocytes by MACS magnetic bead separation ($CD4^+$ T Cell Isolation Kit, CD25-PE Kit, Miltenyi Biotec, Bergisch Gladbach, Germany) to a purity degree of >95%.

Labeling of Primary Cells

Before further experiments, $CD4^+CD25^-$ T cells were labeled with CellTrace Yellow (Life Technologies, Carlsbad, CA) according to manufactures instructions. First, a CellTrace stock solution (5 mmol/L CellTrace in DMSO) was prepared. Then, 1 μL of stock solution was added to each milliliter of cell suspension. This was incubated for 20 minutes at 37°C and protected from light. Next, culture medium (RPMI; Sigma-Aldrich) was added to the cells (5 times the original staining volume) and it was incubated for 5 minutes. Finally, the cells were centrifuged and resuspended in fresh, prewarmed complete culture medium and incubated for ≥10 minutes before further experiments.

Models of Colitis and Colitis-associated Cancer

All animal studies were conducted at the University of Erlangen-Nuremberg and approved by the Institutional Animal Care and Use Committee of the State Government of Middle Franconia. All mice were bred and maintained in individually ventilated cages.

Adoptive Transfer Colitis

Freshly isolated $CD4^+CD25^-$ splenocytes T cells (2.8×10^6) from gender-matched C57BL/6 mice (12 weeks old) were administered intraperitoneally into $RAG^{-/-}$ mice in 200 μL of PBS.[1]

Chemically Induced Colitis and Colitis-associated Cancer

C57BL/6 mice (8–10 weeks old) were obtained from the central animal facility of Erlangen. Colitis and colitis-associated cancer was induced as previously described.[2] For acute colitis, mice received one week of 1.8% dextran sodium sulfate (DSS; MP Biomedicals LLC, Santa Ana, CA) in the drinking water. For chronic colitis, mice were provided with 3 cycles of 1.8% DSS in the drinking water for 1 week followed by normal drinking water for 2 weeks. For colitis-associated cancer, mice were injected with a single dose of the mutagenic agent 7.4 mg/kg azoxymethane (Sigma-Aldrich), followed by 3 similar cycles of 1.8% DSS in drinking water for 1 week followed by normal drinking water for 2 weeks.

Image Reconstruction

To enhance the high-frequency signal of small structures, the acquired signals were divided into 2 frequency bands, 10–30 MHz (low) and 30–90 MHz (high) before reconstruction.[3,4] In the final images, an overlay of the low-frequency reconstruction (red) and high-frequency reconstruction (green) is shown. Additionally, we performed a reconstruction of the frequency band of 85–87 MHz, which filters out anatomic structures with very high frequency content to detect signals that potentially came from the labelled cells.

Motion Correction

For in vivo applications a motion correction processing was applied as previously described by Schwarz et al.[5] Briefly, the algorithm is based on the observation of disruptions of the ultrasound wavefront generated by periodic vertical movements of the melanin-containing skin layer. These disruptions are used to generate a smooth synthetic surface. Subsequently, the offset between these 2 surfaces is used to correct for the relative position of the detector (Supplementary Figure 1).

Image Visualization

For image 3-dimensional visualization, the commercially available software platform Amira (FEI; ZIB, Berlin, Germany) was used. Maximum intensity projections and 3-dimensional images were generated using standard Amira tools. Different frequencies were pseudocolored and overlaid with the software. Images were sharpened using the software provided unsharp mask filter. Single fibroblast cells were highlighted by using the segmentation tool on the image stack in which signals were filtered from 30–90 MHz. All images were adjusted in hue and saturation using Photoshop elements (Adobe, San Jose, CA) on the entire image without adding or changing features.

Multiphoton Microscopy

Ex vivo multicolor multiphoton microscopy with spectral separation was performed on corresponding murine colonic tissues sections as described previously.[6] Briefly, an upright system (TriM-Scope II; LaVision BioTec GmbH, Bielefeld, Germany) equipped with a femtosecond Ti-Sa-laser and a HC Fluotar L25x/0,95 W Visir objective (Leica, Wetzler, Germany) was used to detect signals in 3 photomultiplier tubes: second-generation harmonics at 395–415 nm (collagens, blue); autofluorescence in the ranges of 415–485 nm (NADH, green) and 540–580 nm (FAD, red).

Quantification of Vessel Diameter and Blood Volume

Vessel diameter and volumes were calculated from raw images in triplicate. The blood volume was calculated using

ImageJ 3D manager plugin (public-domain Java-based image processing software; available at https://imagej.nih.gov). Differences were tested with 2-sided Student's t test and $P < .05$ was considered statistically significant.

Quantification of Labeled Primary Cells

For quantification of labelled $CD4^{+}CD25^{-}$ T cells ex vivo and in vivo, the open-source software Icy (version 1.9.1.0) was used. By using the detection plugin 'Spot detector' with adjusted filter settings, bright spots of a certain size that most likely correspond with the labelled cells were automatically counted in the entire image or single regions of interest. For the quantification of bright spots in the multiphoton images, the following settings were used: detected bright spot, Scale 2 90 (3 px) and Scale 3 90 (7px); size filter, 10-3000. For the quantification of bright spots in RSOM images from the reconstruction in the frequency band 85–87 MHz, the following settings were used: detected bright spot, scale 1 (1 px); size filter, 30–60. For comparison of multiple groups, analysis of variance with Bonferroni posttest was used. $P < .05$ was considered statistically significant.

References

1. Powrie F, Leach MW, Mauze S, et al. Inhibition of Th1 responses prevents inflammatory bowel disease in scid mice reconstituted with CD45RBhi CD4+ T cells. Immunity 1994;1:553–562.
2. Neufert C, Becker C, Neurath MF. An inducible mouse model of colon carcinogenesis for the analysis of sporadic and inflammation-driven tumor progression. Nat Protoc 2007;2:1998–2004.
3. Omar M, Schwarz M, Soliman D, et al. Pushing the optical imaging limits of cancer with multi-frequency-band raster-scan optoacoustic mesoscopy (RSOM). Neoplasia 2015;17:208–214.
4. Aguirre J, et al. Nature Biomedical Engineering 2017;1: 0068.
5. Schwarz M, Garzorz-Stark N, Eyerich K, et al. Motion correction in optoacoustic mesoscopy. Sci Rep 2017; 7:10386.
6. Schurmann S, Foersch S, Atreya R, et al. Label-free imaging of inflammatory bowel disease using multiphoton microscopy. Gastroenterology 2013;145:514–516.

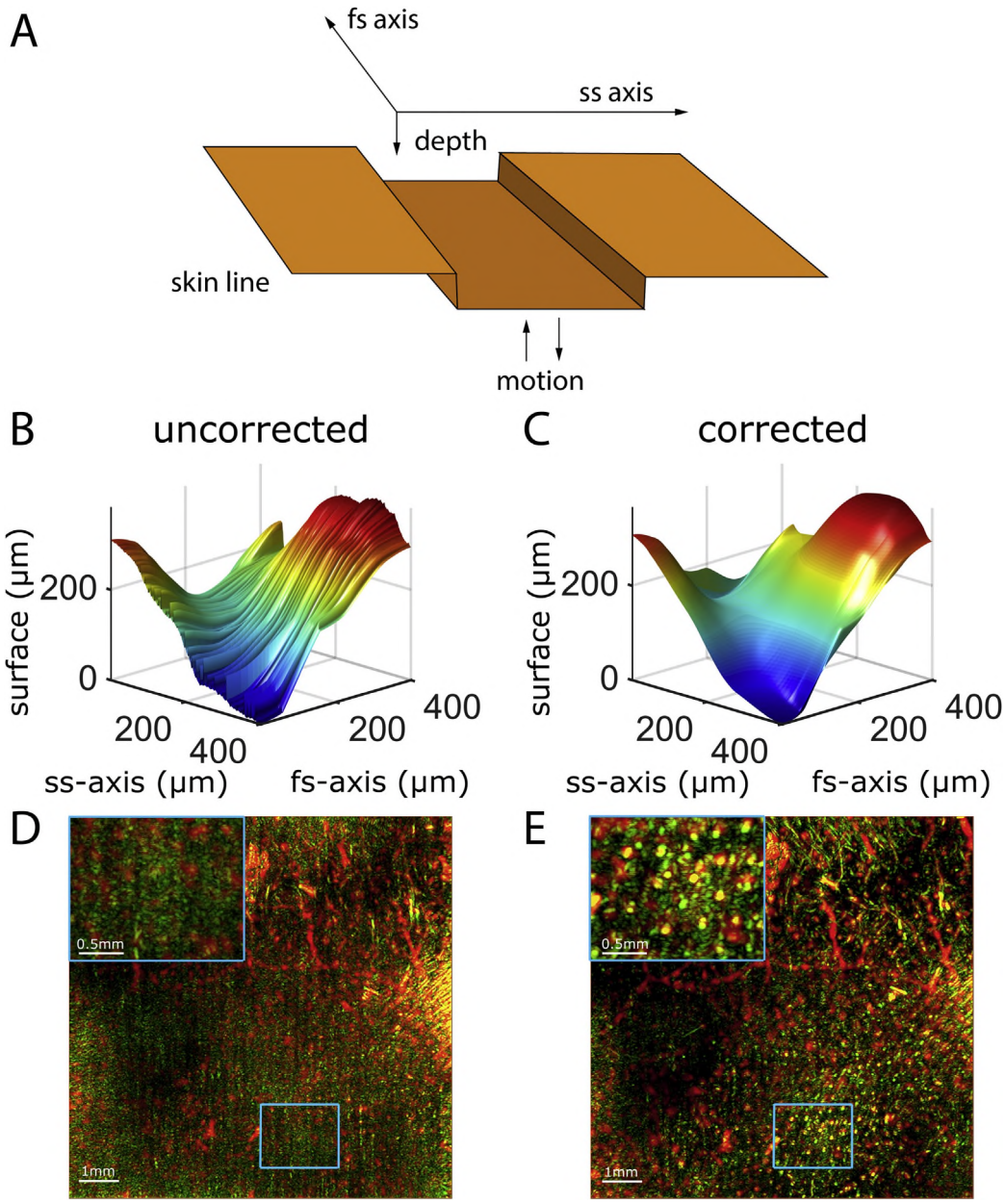

Supplementary Figure 1. (*A*) Schematic overview of dimensional orientation and skin line movements/discontinuation during motion. (*B*) Skin surface raw data before motion correction. (*C*) Skin surface raw data after motion correction. (*D*) Raster-scanning optoacoustic mesoscopy (RSOM) image of murine intestine before motion correction. (*E*) RSOM image of murine intestine after motion correction. Blue boxes indicate area of magnified panel in the upper left corner.